Analysis of the surface termination of $Nd_{1+x}Ba_{2-x}Cu_3O_y$ thin films

X. Torrelles,[1] C. Aruta,[2] A. Fragneto,[5] I. Maggio-Aprile,[3] L. Ortega,[4] F. Ricci,[5,*] J. Rius,[1] M. Salluzzo,[5,†] and U. Scotti di Uccio[5,6]

[1]*Institut de Ciencia de Materials de Barcelona (C.S.I.C.) Campus de la U.A.B., 081893 Bellaterra, Barcelona, Spain*

[2]*INFM-COHERENTIA, Università di Roma "Tor Vergata," Dipartimento di Ingegneria Meccanica, Via del Politecnico 1, 00133 Roma, Italy*

[3]*Département de Physique de la Matière Condensée, Université de Genève, CH-1211 Genève, Switzerland*

[4]*CNRS, Laboratoire de Cristallographie, BP 166, 38042 Grenoble, France*

[5]*INFM-COHERENTIA and Dipartimento di Scienze Fisiche, Università di Napoli "Federico II" Piazzale Tecchio 80, I-80125 Napoli, Italy*

[6]*Di.M.S.A.T., Università di Cassino, Cassino, Italy*

(Received 8 September 2003; revised manuscript received 17 May 2004; published 28 September 2004)

High quality, very flat $Nd_{1+x}Ba_{2-x}Cu_3O_y$ films have been grown by sputtering and analyzed by low energy electron diffraction, scanning tunneling microscopy (STM) and grazing incidence x-ray diffraction (GIXD) employing synchrotron radiation, in order to investigate the surface structure and morphology. The refinement of the GIXD data has been performed on the basis of structural models sensitive to the nature of the terminating layer. The interpretation of the results provides a picture of the surface structure that is in full agreement with STM results. The surface is composed by two terraces with different termination, one of which is an ordered and complete Cu(1)-O layer and the other an incomplete BaO layer that partially covers a disordered Cu(1)-O layer. Atomic vacancies and steps bounding terraces with a height of about 0.4 nm, are present on the surface.

DOI: 10.1103/PhysRevB.70.104519 PACS number(s): 68.35.Bs, 74.78.Bz, 68.55.−a, 74.78.Fk

I. INTRODUCTION

In spite of the enormous amount of work dedicated to the subject, the knowledge of the $R_{1+x}Ba_{2-x}Cu_3O_y$ (RBCO, where R=Y or rare earth) surface structure and termination layer is still far from being complete. This study has a number of technological and fundamental difficulties, also because of the large variety of factors affecting the surface termination, defects, surface relaxation and reconstruction. A noncomprehensive list includes effects related to the substrate choice, the deposition conditions and growth modes, film stoichiometry, strain due to different lattice parameters and expansion coefficients with respect to the substrate, and the interaction with the environment during and after the cooling process.

A great progress in the knowledge of surface properties in connection with film growth modes has been achieved resorting to *in situ* Reflection High Energy Electron Diffraction (RHEED). RHEED studies pointed out that deposition of $YBa_2Cu_3O_7$ (YBCO) films proceeds by unit-cell by unit-cell growth mode.[1] This result would imply a dependence of the terminating layer on the starting monolayer sequence at the interface between the substrate and the film, that may change according to the substrate choice and the termination layer. Such data may complement in some cases the results of surface analyses performed by scanning tunneling microscopy (STM). However, even though atomic resolution has been demonstrated in a few STM measurements,[2] the interpretation of data is troublesome, due to the intrinsic mixing of electronic and topographic information. Moreover the STM measurement is not able to give direct information on the chemical composition of the surface and on the relation between the interface between the surface layers and the bulk.

In this paper, we report on a detailed analysis of structure, microstructure and surface structure of $Nd_{1+x}Ba_{2-x}Cu_3O_y$ (NBCO) films. To this aim, grazing incidence x-ray diffraction (GIXD), low energy electron diffraction (LEED) and scanning tunneling microscopy data have been collected and analyzed. The GIXD experiment has been carried at the ID32 beamline of the European Synchrotron Radiation Facility (ESRF) in Grenoble. In order to get meaningful surface characterization, we faced the problem of possible aging or contamination of the samples, which have been grown in an Ultra High Vacuum (UHV) deposition system not connected *in situ* to the UHV surface diffraction chamber. Our previous experience, corroborated by similar studies performed by other groups,[3,4] proved that suitable thermal treatments can restore the surface structure of RBCO *c*-axis films as demonstrated by LEED. Similar treatments have been adopted in this work.

The choice of $Nd_{1+x}Ba_{2-x}Cu_3O_y$ for our investigation, instead of the more popular $YBa_2Cu_3O_7$ compound, is due to the different surface morphology of this material. One intrinsic characteristic of YBCO *c*-axis films grown by various techniques is that, after few layers, 3D islands are formed. Such structures are made up of stacks of terraces 1 unit cell high. Relaxation can be one of the main reasons for the crossover from a 2D to a 3D growth mode, but also other mechanisms have been proposed to explain this phenomenon.[5] YBCO surfaces show therefore a substantial roughness that is a clear obstacle for the determination of the surface structure using electron diffraction or x-ray surface diffraction. However, the growth mode of $Nd_{1+x}Ba_{2-x}Cu_3O_y$ is different. A 2D-nucleation growth mechanism has been demonstrated for such films, when grown by sputtering from a single target.[6] STM measurements proved the existence of

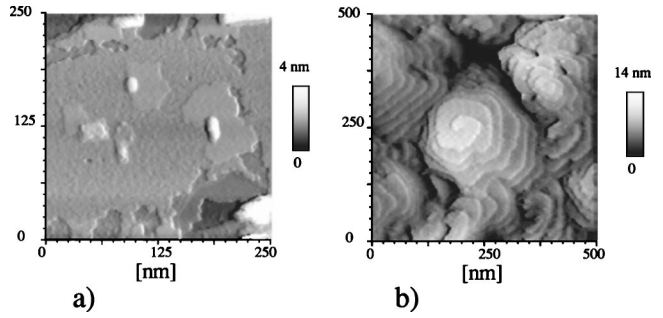

FIG. 1. STM topography images of (a) a 100 nm thick $Nd_{1+x}Ba_{2-x}Cu_3O_y$ film and of (b) a 50 nm thick YBCO film deposited on a $SrTiO_3$ substrate. The images are taken in the constant current mode with electrochemically etched iridium tips, tunneling current of 300 pA and tunneling voltage of 1.2 Volts.

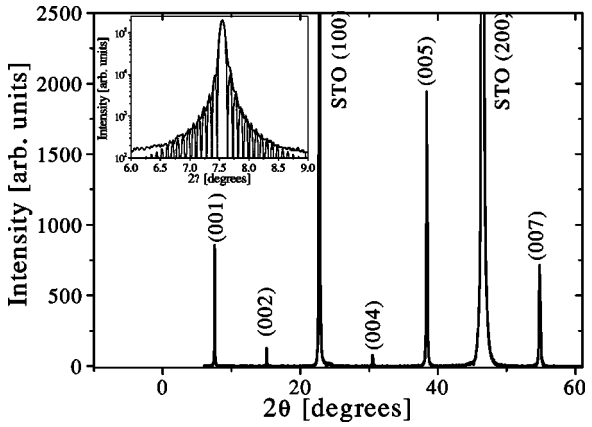

FIG. 2. ϑ-2ϑ scan of a typical sample. The inset shows well defined pendellösung fringes around the (001) reflection.

2D-terraces separated by steps with height even less than 1 unit cell.[7] As a consequence, NBCO films have a superior flatness with respect to YBCO. A comparison between the morphology of a 100 nm thick $Nd_{1+x}Ba_{2-x}Cu_3O_y$ film and of a 50 nm thick YBCO film is shown in Fig. 1. The UHV-STM images are taken *in situ* on as grown samples in the constant current mode, using an electrochemically sharpened iridium tip.

The microstructure of Nd-rich $Nd_{1+x}Ba_{2-x}Cu_3O_y$ films was previously investigated by HREM (High Resolution Electron Microscopy), and compared with that of stoichiometric $NdBa_2Cu_3O_7$, with the aim of determining the location of the excess Nd ions in the structure, and the related defects that are originated.[8] It was demonstrated that in Nd-rich films, Nd-excess is incorporated in two ways: by forming $Nd_2Ba_2Cu_4O_y$ 224-type stacking faults, which in less extent are observed also in stoichiometric YBCO films, and by the introduction of extra (Nd-CuO_x) blocks. In the Nd-rich samples far more Anti-Phase Boundaries (APB) are formed due to the enhanced Nd-Ba exchange. Some APB's are preserved up to the surface and do not end at a dislocation, while others are annihilated without the formation of linear defects through the introduction of extra (Nd-CuO_x) blocks. This mechanism allows a further incorporation of the Nd in the $Nd_{1+x}Ba_{2-x}Cu_3O_y$ matrix, and partially explains the superior flatness of these films.[8]

In the next section, the sample's fabrication and characterization are presented. The remaining part of the paper is then dedicated to the description of the experiment at the ESRF, to the analysis of the structural data, and finally to the discussion of the results.

II. SAMPLE FABRICATION AND CHARACTERIZATION

The high quality $Nd_{1+x}Ba_{2-x}Cu_3O_y$ (NBCO) thin films have been grown by dc magnetron sputtering, using a single target with $Nd_{1.1}Ba_{1.9}Cu_3O_y$ stoichiometry. $Nd_{1+x}Ba_{2-x}Cu_3O_y$ films were deposited on 5×5 mm^2 wide, (100) $SrTiO_3$ (STO) substrates. Before the deposition the substrates were annealed for one hour at 950 °C in vacuum. Such thermal treatment provides a clean surface, mainly TiO_2 terminated, as revealed by lateral AFM friction measurements and previous studies.[9] The sputtering takes place in an $Ar+O_2$ atmosphere with a partial pressure ratio $P(Ar):P(O_2)=20:1$ and total pressure in the range 40–60 Pa. The deposition temperature is 740 °C for the samples considered in this work, with a growth rate of 0.02 nm/s. After deposition the films are annealed for one hour at 480 °C, in pure oxygen (99.998%) at 3×10^4 Pa.

We estimated by EDX (Energy Dispersive X-ray) and XPS (X-ray Photoemission Spectroscopy) analyses that the Nd/Ba ratio in the film used in this study is 0.62 ± 0.03, which is slightly larger than in the target (Nd/Ba=0.58). The $Nd_{1+x}Ba_{2-x}Cu_3O_y$ *c*-axis length is known to be related to the Nd/Ba ratio in films[10] and in bulk samples.[11] The estimation of the Nd/Ba ratio based on x-ray measurements of the lattice parameter is however consistent with the target stoichiometry within the experimental uncertanties. Such $Nd_{1+x}Ba_{2-x}Cu_3O_y$ films are superconductors, and due to the relatively high Nd content show a relatively low transition temperature ($T_c=64$ K,$\Delta T_c=3$ K). While it is possible to optimize the critical temperature of sputtered NBCO films,[6] our choice for a relatively lower T_c film is dictated by the better surface morphology and structure as shown below.

The structural and morphological properties of the samples were investigated by *in situ* UHV scanning tunneling microscopy, and by x-ray diffraction measurements. X-ray diffraction spectra always show a high degree of *c*-axis epitaxy. Most of the samples exhibit well defined Pendellösung fringes in the ϑ-2ϑ scan on the (001) reflection (Fig. 2) that allow a careful determination of film thickness.

In Fig. 3(a) it is shown a magnified image of the surface of a Nd-rich NBCO film. The surface is composed by terraces with different topography separated by steps. Each terrace is between 50 and 80 nm wide. Some terraces are very flat, while others show a rms (root mean square) roughness of about 0.2 nm as shown in the height profile of Fig. 3(b). This is about the same value as the distance between two neighbor atomic layers along the *c*-axis in the $Nd_{1+x}Ba_{2-x}Cu_3O_y$ structure. Consequently, rough terraces may be incomplete layers and the second surface layer may be also partially exposed at the surface.

More details on the results of the STM measurements and on the fabrication technique of $Nd_{1+x}Ba_{2-x}Cu_3O_y$ films have been reported elsewhere.[5,7]

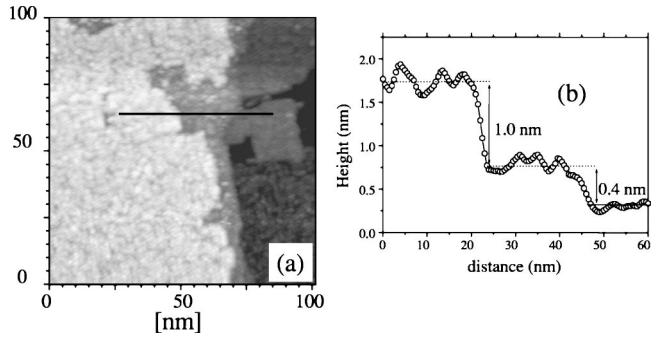

FIG. 3. The magnified STM image of the surface of a 60 nm $Nd_{1+x}Ba_{2-x}Cu_3O_y$ film (tunneling current of 200 pA and bias voltage of 1.0 Volts) (a) and height profile along the line showing the rough and flat terraces (b).

In order to perform the structural investigation with the synchrotron radiation, the samples must be transferred from the deposition chamber to the synchrotron beamline. The as grown films used for the experiment were introduced at a pressure lower than 10^{-5} Pa to a fast-entry intro-chamber. Here the samples were hermetically sealed in a glass container filled with ultra-high purity Ar gas (99.998% pure). The effect of aging and contamination of the surfaces of the samples after such exposure to the atmosphere has been investigated by low energy electron diffraction (LEED). The LEED analysis has been performed *in situ* on as-deposited samples and on treated samples. *In situ* LEED on as-grown films has shown that the surface of $Nd_{1+x}Ba_{2-x}Cu_3O_y$ exhibit a $c(2\times2)$ reconstruction (Fig. 4). This is different from the $p(2\times2)$ surface reconstruction of $NdBa_2Cu_3O_7$ (Ref. 12) and $YBa_2Cu_3O_7$.[4] The LEED pattern of films exposed to the ambient atmosphere for 1 minute is completely degraded, and only exhibits an isotropic diffuse intensity. This effect can be related to the well known contamination of RBCO by water vapor and carbonates.[13] These contaminants are however eliminated by annealing the sample in 50 mTorr of molecular oxygen at 500 °C for 30 minutes. *In situ* XPS performed in an ESCALAB system connected *in situ* to the LEED and preparation chamber,[14] shows that in the RBCO samples, chemical film properties and surface morphology[15] are not affected by this annealing procedure. After such a thermal treatment, the LEED pattern is restored even in the case of samples kept in a controlled atmosphere for more than two weeks. This treatment has therefore been adopted for the sample used for the GIXD experiment, in a specially designed UHV chamber connected to the UHV diffraction chamber, kept at a pressure below 10^{-7} Pa.

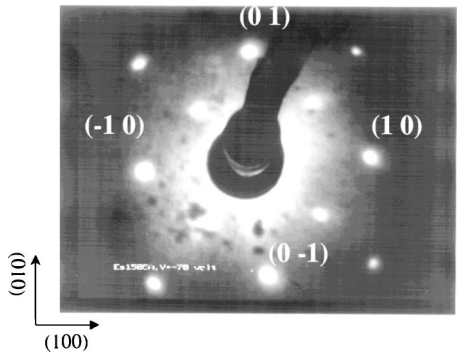

FIG. 4. The LEED image showing the $c(2\times2)$ reconstruction of a $Nd_{1+x}Ba_{2-x}Cu_3O_y$ film after exposure to the air and annealing procedure.

III. GIXD EXPERIMENT

The surface x-ray diffraction experiment was carried out at the ID32 surface diffraction and standing waves beamline at the ESRF. The incoming x-ray beam was generated by two undulators and monochromatized with a Si(111) double crystal monochromator, cryogenically cooled,[16] that was set to an energy of 13.9 keV at the 5th harmonic of the undulator. The whole UHV surface diffraction chamber is mounted on the 2+2 circle goniometer. Additional motors that allow the sample surface alignment by changing the height of the sample respect the direct beam, and tilting in the x and y directions are located in the chamber.

The $Nd_{1+x}Ba_{2-x}Cu_3O_y$ film employed in this experiment is composed of 52 unit cells. Before performing the GIXD measurements, the structural quality of the sample was checked from the rocking curves of several reflections. The (−1, 0, 1) and (0, −3, 1) rocking curves exhibit a FWHM (Full Width Half Maximum) of 0.05° and 0.03°, respectively. We have experimentally determined the critical angle ϑ_c for our sample. During the GIXD data acquisition procedure the angle of incidence of the x-rays to the surface was consequently kept constant at 0.375°, which is slightly higher than the measured value of $\vartheta_c=0.360°$. This rather low incidence angle was selected in order to enhance the signal to background ratio coming from the surface, and to minimize contributions of the substrate to the diffracted intensity.

The film lattice parameters were determined from the refinement of 12 film bulk reflections by least-square procedures. In order to avoid the contribution of the substrate, we have chosen film bulk reflections which are far from the substrate peaks. For example the (1 0 1) substrate reflection is superimposed to the (1 0 3) film reflection and for this reason has been discarded in the fit refinement. Using this procedure the final values of the cell parameters were $\mathbf{a}_1=\mathbf{a}_2=0.3902(1)$ nm, $\mathbf{a}_3=1.1730(1)$ nm, $\alpha=\beta=\gamma=90.0°$. The lattice parameters of the $Nd_{1.1}Ba_{1.9}Cu_3O_y$ starting target are $a=0.3912(1)$ nm, $b=0.3865(3)$ nm, and $c=1.1725(1)$ nm. Thus, the film has lattice parameters that slightly differ from the target ones. Moreover, the target unit cell is orthorhombic while the film one is pseudo-tetragonal. This effect may be accounted for by a slight difference in composition and by the strain induced by the substrate as discussed in the following.

As reported in the previous section, the composition measurements performed by XPS and EDX indicate that the ratio between Nd and Ba is given by $Nd/Ba=0.62\pm0.03$ for the investigated sample. X-ray measurements proved that this film possesses a tetragonal unit cell and is untwinned. This is certainly an intrinsic property, and cannot be related to oxygen loss. In fact, tetragonal RBCO structures are found for very low oxygen contents, which implies sensitive expansion

of the *c*-axis and a consequent contraction of the *a* and *b* axes; this is not the case of our film, which has a shorter *c*-axis (1.1730 nm compared to the 1.1745 nm value for the *c*-axis of a stoichiometric NBCO film) and *a* and *b* axes similar to the substrate. On the contrary, the tetragonal structure may be due in this case to the combined effect of excess oxygen and strain at the interface with the substrate. When an excess Nd^{3+} is inserted in the structure, charge neutrality is satisfied allowing some more O^{2-} ions in the free sites of the Cu(1)-O planes. This effect has been demonstrated in NBCO bulk samples by neutron diffraction.[17] In particular it has been established that for each two Nd^{3+} in excess, one oxygen ion is added at the anti-chain sites and at the same time a reorganization of the remaining oxygen in the structure leads to a gradual destruction of the chains and finally to an orthorhombic to tetragonal transformation for $x=0.25$. For our Nd/Ba=0.62 value we get $y=7.1$, which is an excess of 0.1 O-ions per unit cell. While the *b*-axis of our film is not much different from the expected value for this composition, the *a*-axis, which is actually equal to the *b*-axis, is unexpectedly high. This result suggests that oxygen ions are added at the anti-chain sites. Moreover the film is subject to strain induced by the substrate. As a consequence the *a* and *b* axes of the film are similar to that of the substrate and the in-plane axes of the $Nd_{1+x}Ba_{2-x}Cu_3O_y$ film resulted parallel to the principal axes of the $SrTiO_3$ substrate.

Before collecting data, we have defined an orientation matrix through the base vectors $(\mathbf{b}_1,\mathbf{b}_2,\mathbf{b}_3)$ of reciprocal space chosen as follows: $\mathbf{b}_1//[100]$ film; $\mathbf{b}_2//[010]$ film; $\mathbf{b}_3//[001]$ film, with $\mathbf{b}_1$,$\mathbf{b}_2$ lying parallel to the substrate surface. Their amplitudes have been chosen according to the determined lattice parameters of the film, i.e., $\mathbf{b}_1=2\pi/\mathbf{a}_1=\mathbf{b}_2=2\pi/\mathbf{a}_2=16.09\ \mathrm{nm}^{-1}$, and $\mathbf{b}_3=2\pi/\mathbf{a}_3'=16.06\ \mathrm{nm}^{-1}$, where $\mathbf{a}_3'=\mathbf{a}_3/3$. Notice that the length of $\mathbf{b}_3$ has been defined with respect to the *c*-axis of the $Nd_{1+x}Ba_{2-x}Cu_3O_y$ film divided by 3. According to this definition, a vector of the reciprocal space is denoted in the following as $h\mathbf{b}_1+k\mathbf{b}_2+l\mathbf{b}_3$.

Two different sets of reflections have been collected: integer and fractional order rods. A total of 1929 reflections were measured, which reduced to 1617 nonequivalent intensities corresponding to 28 fractional order rods and 6 crystal truncation rods (CTR). The analysis of the data related to the fractional order rods will be discussed in a separate paper, and are not reported here. We wish only to mention that the surface of our sample is characterized by $c(2\times2)$ reconstructed domains about 50 nm wide, as inferred from the angular widths Δh and Δk of the $(\frac{1}{2},\frac{1}{2},0.15)$ reflection. The $(\frac{1}{2},\frac{1}{2},0.15)$ reflection intensity was periodically measured for checking anomalies during the data collection procedure. The systematic errors resulting from sample misalignments were checked by measuring several rods from all four quadrants in reciprocal space.

The exploration of the reciprocal space of the film has been performed as follows. The CTR's were collected by the subsequent acquisition of ω-scans at different values of *l* for each fixed (h,k) value. Here ω refers to the degree of freedom of the sample concerning a rotation around the axis perpendicular to the surface. An *l*-spacing of 0.05 rlu (reciprocal lattice units) has been adopted. As an example, we have plotted in Fig. 5 the ω-scans around the $(1,1,l)$ reflection from which the (1,1) CTR has been determined. Each ω-scan is integrated, and geometrical corrections are implented according to Ref. 19 in order to obtain the intensity profile of the six (h,k) integer order rods.

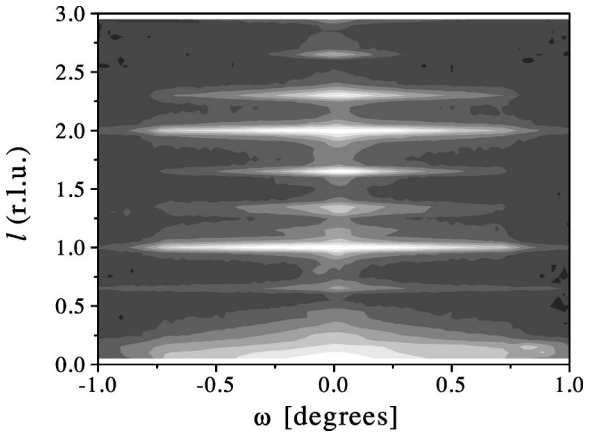

FIG. 5. Contour plot of the scattered radiation at $(h=1,k=1)$ obtained through ω-scans at various values of *l*.

IV. RESULTS

The calculations of CTR's intensities have been performed using a modified version of the ROD software program.[18] Due to the high complexity of the structure, the fit of the experimental data required a number of intermediate steps. In the preliminary fitting sessions, a reduced number of parameters was introduced to get the overall physical picture; moreover, these analyses also allowed us to check the sensitivity of the fit to specific sets of parameters. The route toward the final structural description is discussed in the following.

A. Ideal truncated crystal model

Figure 6 shows the comparison between the simulations obtained from an ideal NBCO truncated crystal with the experimentally corrected intensities[19] measured at several *l*-values related to different integer order reflections. The differences between the various simulated curves in Fig. 6 are due to the different surface terminations, which are in principle possible for this kind of material. Each possible plane, that is Cu-O (chain layer), Ba-O, CuO_2 (copper-oxide layer) or Nd, was considered. As clearly shown in each of the subset figures of Fig. 6, none of the theoretical curves agree with the experimental results, showing that the surface structure is different from the ideal one. The most striking feature of the intensity shape profile of the different ideal surface terminations calculated in Fig. 6 is the abrupt variation around the Bragg peaks located at low *l*-values, i.e., CTR(1,0) $l=1$. The experimental measurements, instead, show smooth intensity changes around these peaks. Moreover weaker peaks between the Bragg points can be distinguished in some of the measurements shown in Fig. 6. In the following we will show that they are related to the $c(2\times2)$ surface reconstruc-

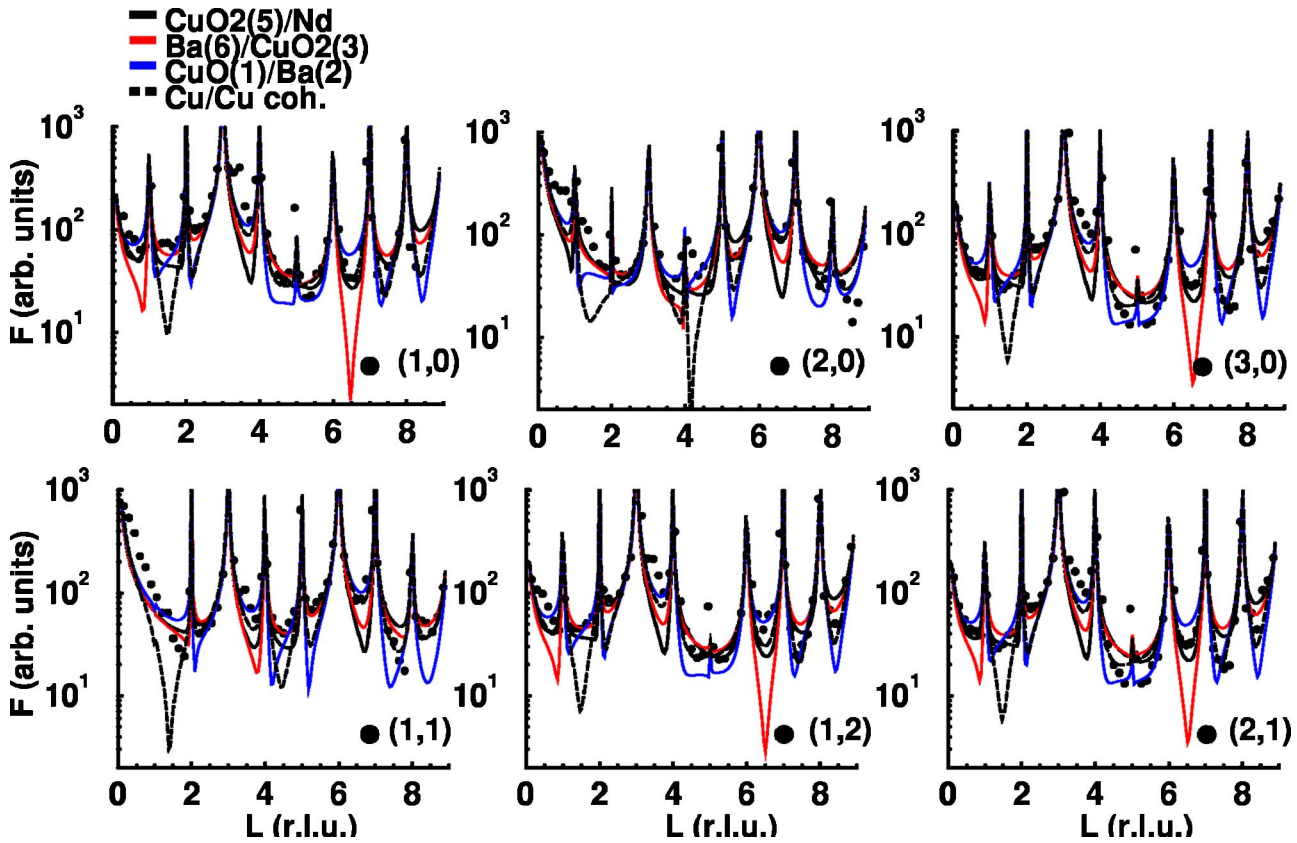

FIG. 6. A comparison between experimentally corrected intensities at different Bragg points (h,k) as a function of 1 (CTR's) and calculated curves relative to different ideal surface terminations of the NBCO film. The experimental error bars have been omitted for clarity. Filled circles correspond to the experimental data while continuous lines are the simulations: black line corresponds to Cu(5)-O_2 *or* Nd(4) termination, the blue line Cu(1)-O or Ba(2)-O termination, the red line Ba(6)-O or Cu(3)-O_2 termination and a black dashed line corresponds to a coherent superposition of two Cu(1)-O layers separated along the surface normal by two layers (0.4 nm). The notation used is the same shown in Fig. 7.

tion. All these features cannot be reproduced by a simple bulk termination structural model.

In the following we will consequently consider two models for the NBCO film surface: (i) a regular film surface having only one kind of termination with the possibility of a random substitution of Ba atoms on Cu sites in its topmost surface layer. In this case the distribution of steps bounding terraces is parametrized by a roughness coefficient. (ii) A surface formed of two differently terminated domains involving atomic layers of different heights and separated between them distances smaller than the coherence length of the x-rays. From the STM measurements [Fig. 3(a)] it is evidenced that the surface is composed of terraces with different heights and separated between them around 50–80 nm. Consequently the total diffracted intensity can be due to the coherent contributions from the different regions.

B. Single termination model

In order to fit the GIXD data, as a second step, we developed a coherent, single termination, model of the sample structure. A different level of complication is gradually introduced in this model in order to understand the effective role of ion relaxation, chemical disorder, surface termination and roughness.

1. Ion relaxation and chemical disorder

The film is considered as a stack of unit cells. Starting from the interface with vacuum, we consider nine independent unit cells to take into account surface normal atomic relaxations of the outermost part of the film, plus a bulk unit cell (collection of identical cells), which represents the inner part of the sample. We have also taken into account the pos-

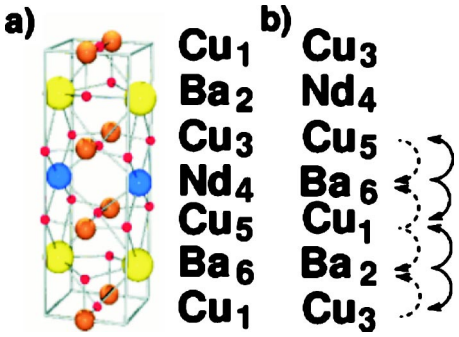

FIG. 7. (a) Basic NBCO unit cell used to build the model. Red small spheres correspond to the oxygen atoms. (b) Scheme showing the Cu/Ba exchange distribution that preserves the film stoichiometry.

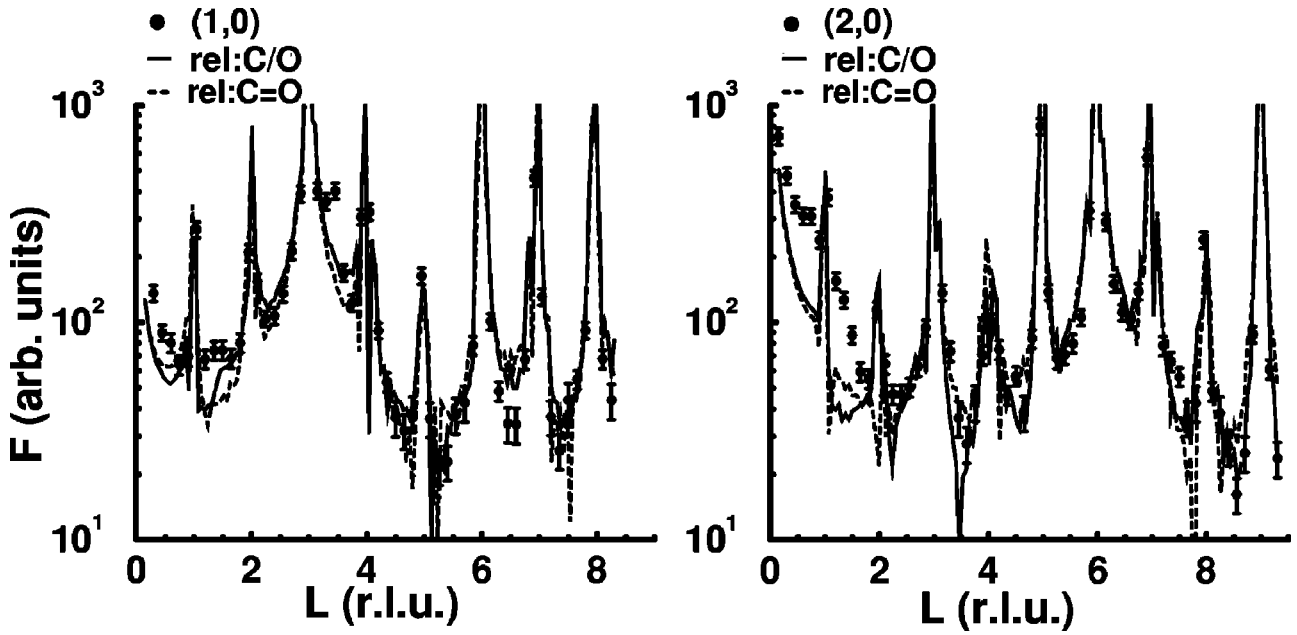

FIG. 8. A comparison between the experimental results relative to the (1,0) and (2,0) (filled circles) CTR's and the single termination model fit obtained by considering relaxation of the cations with oxygen positions coupled to the correspondent cations (dashed line) and the model which consider the oxygen free to relax (continuous line).

sible contribution associated to the $SrTiO_3$-NBCO interface. In our analysis we checked both incoherent and coherent interface contributions to the total CTR. The best agreement, for any of the models presented below, was always obtained when the contribution coming from the $SrTiO_3$ is incoherent. The incoherent contribution from the substrate was estimated from the fits to be 25%. A schematic drawing of the starting structural model is shown in Fig. 7. In each cell, the vertical coordinates of ions are free fitting parameters. To account for the presence of defects, we have also allowed some degree of ion substitution (chemical disorder). Since the atomic scattering factors of Nd and Ba are similar, the intensity of the scattered x-ray radiation is not sensitive to small changes in the effective Nd/Ba ratio of the sample. Moreover, oxygen gives a minor, but not negligible, contribution due to its low atomic number.

At first, the positions of oxygen ions are coupled to those of the cations of the same layer while the chemical ordering of the film is maintained. The maximum number of fitting parameters involved in this model is 55 (1 scale factor and 54 parameters corresponding to the cations *z*-coordinates).

Surface termination plays an important role in the fit. Therefore we have again considered all possible surface terminating layers during the fit refinement procedure. In Fig. 8 are shown the results of the fit for the (1,0) and (2,0) CTR's (dashed lines). The best agreement in terms of χ^2 is obtained for Cu(1)-O terminated layer. As shown in Fig. 8, the improvement of the model which consider surface relaxation compared to the ideal structure is obvious. When the oxygen positions are also permitted to relax by including 45 extra parameters the fit improves considerably (continuous lines in Fig. 8).

Finally the Cu and Ba occupancies in each layer are treated as free parameters to account for a possible chemical disorder of the film. During the fit refinement procedure the overall chemical stoichiometry of the film is fixed. This means the addition of 18 new parameters to the model. Figure 7(b) shows a schema of how this Cu/Ba substitution is taken into account. In the best fit, the average substitution between Cu and Ba along the surface normal direction is about 6%. In spite of the extra occupancy parameters added to the model, no real improvement of the fit was observed, since it gives similar fitting curves to those of Fig. 8 (cation+oxygen relaxations) and a higher value of χ^2. Therefore we decided to neglect the Cu/Ba substitution in the next, except for the outermost film layer.

2. Surface roughness

As third step Cu/Ba exchange in the topmost unit cell is introduced in the model and roughness has been parametrized. The roughness should be introduced in the model, since our film, even being quite smooth, is composed by

TABLE I. χ^2 values obtained from the fit of the experimentally measured CTR's using the refined structural single termination model. Each possible termination has been considered. The best agreement is obtained for a Cu(1)O layer termination containing a 30% of Ba ions at the Cu site.

Termination layer	χ^2
Cu(1)-O	8.4
Ba(2)-O	9.0
Cu(3)-O_2	10.2
Nd(4)	9.6
Cu(5)-O_2	8.5
Ba(6)-O	9.1

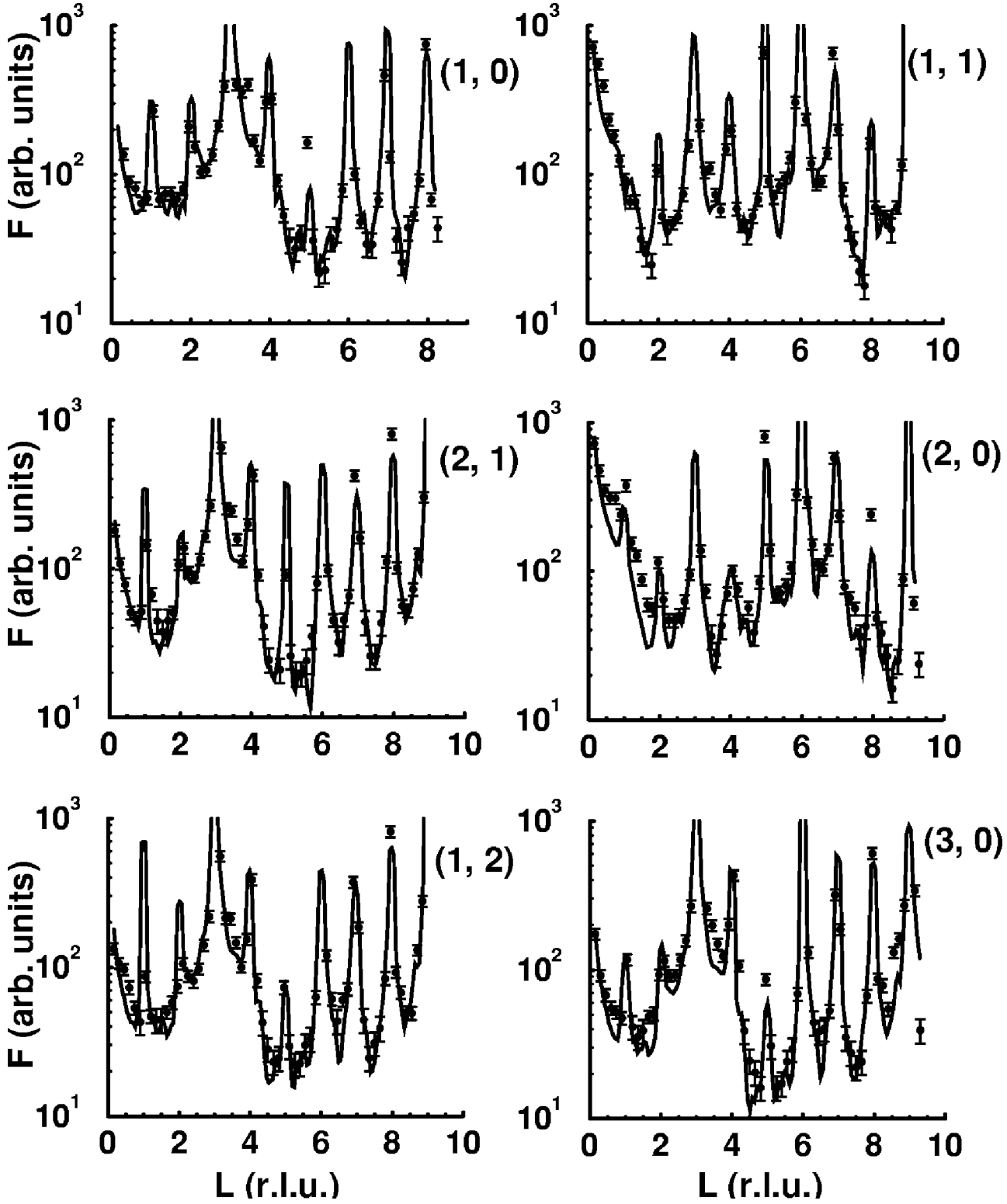

FIG. 9. A comparison between the single termination model best fit and the experimental data taking into account cation/oxygen relaxations, substitution of Ba in the Cu(1) position at the topmost surface layer and surface roughness.

terraces separated by single and, sometimes, multiple steps. We used a step of one NBCO unit cell to compute the surface roughness within the beta-model.[21] This choice gives the best agreement between the data and the models. The Cu-Ba exchange at the surface is physically much more reasonable since during sputtering each species is supplied at the same time on the position of the substrate. This is different from the deposition by atomic layer by layer molecular beam epitaxy technique. Again each possible terminating layer has been considered in this refinement. In Table I we report the

χ^2 obtained from the fit to the structural model which considers (i) 9 surface unit cells with (ii) cation and oxygen atomic relaxations not forced to be identical and (iii) Cu/Ba substitution at the topmost surface unit cell, as well as roughness. As clearly shown in Table I the best results in terms of χ^2 are obtained for a Cu(1)-O terminated surface layer, being characterized by a 30% amount of Ba substitution at the Cu site. Figure 9 shows the comparison of the best fit with the experimental data using this model. The differences between the fits shown in Figs. 8 and 9 are noteworthy and are only due to parametrization of the surface roughness and to the Cu/Ba substitution on the topmost surface layer. From the results displayed in Fig. 9 the topmost surface layer is mainly Cu(1)-O terminated ($\simeq$70%) with approximately 30% of Ba substitution on Cu sites. It is worth mentioning that the β value obtained from the fit correspond in this case to a rms roughness of 0.1 nm, which disagrees with the maximum rms roughness of 0.2 nm observed by STM for some terraces.

Another remarkable result is that a considerable displacement toward the surface of the cations *z*-positions is obtained from the fit. As shown in Fig. 10 the average displacement is maximum for the outermost surface layers (which reach a maximum of 20% approximately) and progressively diminishes to zero with depth. In spite of such a large displacement of each surface layer from its ideal position, the average interlayer spacing is very close to that of the ideal NBCO film (open circles in Fig. 10). The behavior of the average oxygen displacements is different from that of cations in the three topmost surface unit cells. This different behavior for both types of displacements could be related to the fact that one type of atom (cations or oxygen) must be the main one responsible for the $c(2\times2)$ reconstruction and consequently must be more sensitive to their contributions in the CTR's.

C. Coherent, two termination, model

As shown in the previous section a model with a single terminated surface is able to fit the experimental data, supposing that (a) there is a strong relaxation of both cations and oxygen ions in the 9 topmost surface unit cells; (b) the surface is Cu(1)-O terminated ($\simeq$70%) with approximately 30% of Ba substitution on Cu sites. However we have also noted that a coherent superposition of CuO and BaO surface terminating layers may smooth out the abrupt variations around the main Bragg peaks present in the ideal truncated crystal model, which is actually not observed in the experimental data. This means that by using a coherent superposition of Cu(1)-O and BaO surface layers in place of a single termination model, it is possible to reproduce the experimental data without involving strong relaxation of the topmost 9 unit cells.

From the STM inspection of the surface morphology in Fig. 3, we have seen that the NBCO surface is composed of two kinds of terraces: one of which characterized by a rms roughness of about 0.2 nm, the other being atomically smooth. For this reason we consider a structural model for the surface as suggested by the STM results. In this model we just suppose that the surface is composed by two kinds of

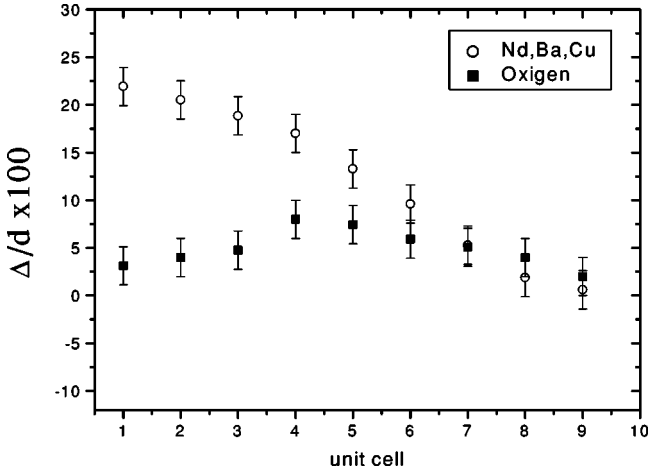

FIG. 10. Average layer displacement, obtained from the single termination model, from its ideal position for each unit cell corresponding to cation displacements (open circles) and oxygen displacements (filled squares). *d* is the interlayer distance of the NBCO unit cell ($a_3/6$) and Δ the variation with respect to this value.

terraces, with different terminations, which contribute coherently to the full diffracted intensity along the CTR's. The height distance between these terraces is changed in each fit procedure according to the termination layers. Moreover we have taken into account relaxation of the last 4 unit cells by introducing extra parameters for the ion displacement along the surface normal. Finally we have added a new parameter which takes into account the disorder along the whole film (surface and bulk) in the form of a global Debye Waller factor. The number of parameters in this model is strongly reduced to 60 (30 *z*-parameters for cations, 25 for oxygen atoms, one global Debye-Waller factor, 2 occupancy parameters, one scale factor and one roughness parameter) compared to the previous model being characterized by 103 parameters. In Fig. 11 we show the result of the best fit for the new model, which is obtained supposing a surface that mainly contains two terraces, each of them covering the same portion of surface. The surface termination of one of the terraces seems more ordered than the other since one of them is exclusively Cu(1)-O terminated while the other shows a distribution of vacancies and disorder in the two topmost layers: from the fit it is evinced that the topmost surface layer is a partially filled BaO layer (50%) while the second layer is Cu(1)-O with a random substitution of Ba by Cu atoms (50:50). The separation distance between the Cu(1)-O and BaO topmost surface layers from both domains is of one atomic layer (0.2 nm). In spite of the much-reduced number of parameters, the χ^2 is reduced to 5.2. By supposing the oxygen ions in each atomic layer coupled to the cations (that means only 35 parameters in the model) the χ^2 increases only slightly ($\chi^2=6.2$), remaining well below the value obtained within the single termination model. It is worth noting that any other pair of surface terminations gives χ^2 values systematically larger. In Table II the results obtained from some of the fitting attempts, taking into account the possible termination layers for regions I and II characterized by the different separation between respective topmost layers, are shown. Moreover from the several possible sur-

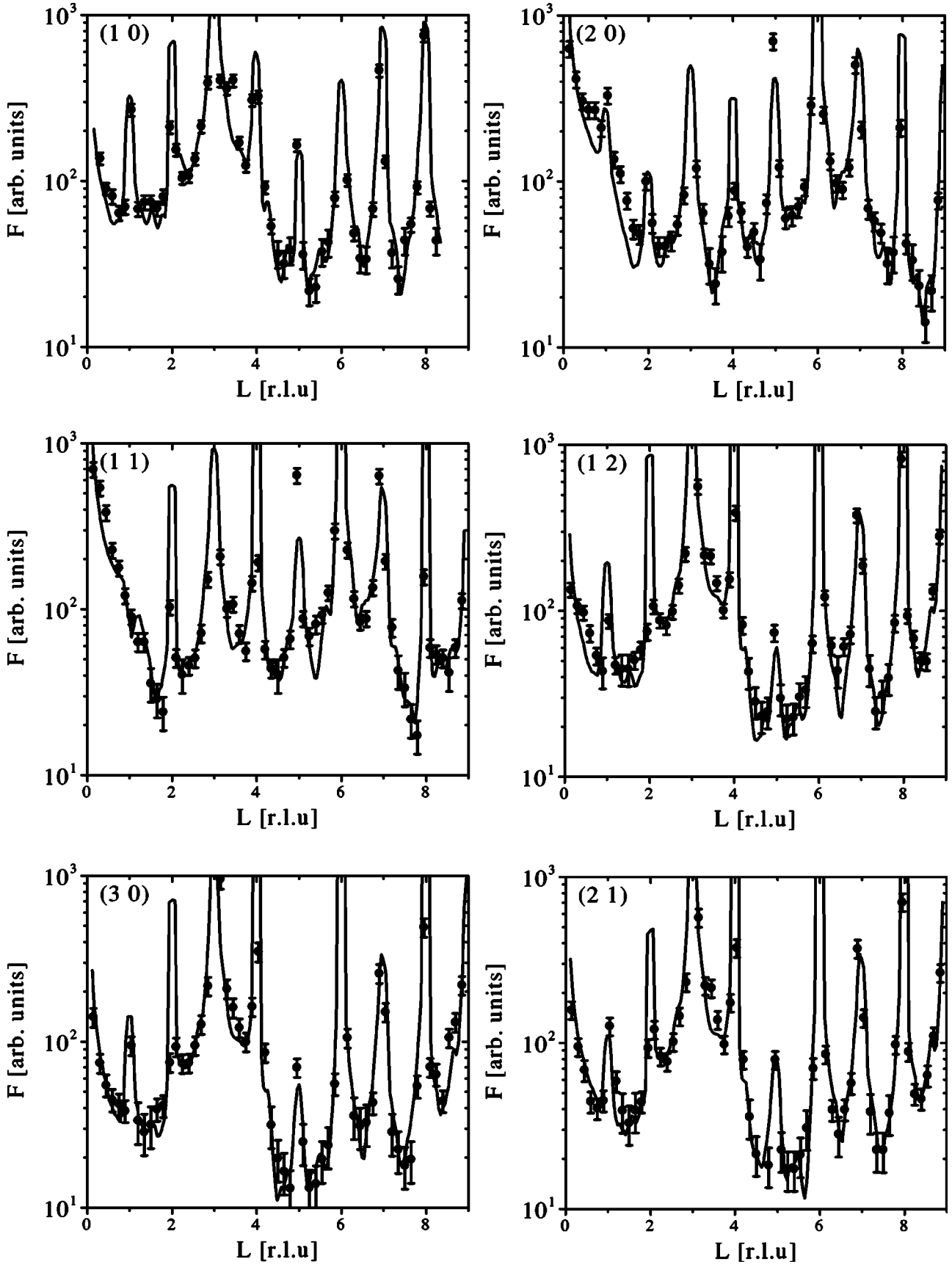

FIG. 11. A comparison between the two termination model best fit and the experimental data as described in the text.

TABLE II. χ^2 values obtained from the fit in the two terminations models. The two coherent domains are designed as regions I and II. The difference in height between the topmost layers (T.L.) from both regions I and II is expressed in terms of the separation distance as depicted in Fig. 13. Other surface terminations as CuO_2 or Nd were also checked and gave χ^2 values larger than 9.

Region I	Region II	Separation distance (monolayers) (1 monolayer=0.2 nm)	χ^2
BaO (T.L.)	BaO (50%) (T.L.) Cu/Ba (50:50) (2nd L.)	0	7.0
BaO (T.L.)	Cu/Ba (50:50) (T.L.)	1	7.3
CuO(1) (T.L.)	CuO(1) (T.L.)	2 or 1	8.6 or 8.5

face terminations which we have considered in this model the best fit is always obtained for terraces which have a difference in height between the topmost full surface layers of two atomic layers (0.4 nm).

It is interesting to observe that both models give similar quantitative results concerning the average chemical composition of the surface termination. From the occupancies of their respective topmost layers, the single termination model provides a Cu/Ba ratio at the interface with a vacuum of about 2.3 while in the coherent superposition of two surface domains model it is 1.7.

Concerning relaxations of the last unit cells, it is important to underline that the displacement of the ions obtained from the fit is much less pronounced compared to the previous model, as expected. In Fig. 12 we show the ion displacement obtained in the best fit for cations and oxygen ions. It is remarkable that also in the two terminations model the cation relaxation is opposite to the oxygen ones in the topmost surface layers, i.e., cations tend to displace along the surface normal, while oxygen ions have an opposite behavior. This different result for both types of displacements can be again interpreted as related to the fact that one type of atom (cations or oxygen) must be the main one responsible for the $c(2\times2)$ reconstruction and consequently must be more sensitive to their contributions in the CTR's. Concerning the relaxation of the last surface cell it is remarkable that the complete CuO surface termination layer is contracted while the other is expanded. This result can be related to the more disordered structure of the topmost surface layers. The calculated roughness of the film is approximately one atomic layer. The β value[20] is 0.15, which corresponds to a root-mean-square elevation of the surface contour of 0.1 nm. The film disorder introduced as a global film thermal vibration parameter corresponds to an average isotropic disorder of 0.02 Angstroms in the positioning of each atomic layer.

In Fig. 13 a schematic diagram of the surface structure which emerges from the two terminations model is depicted.

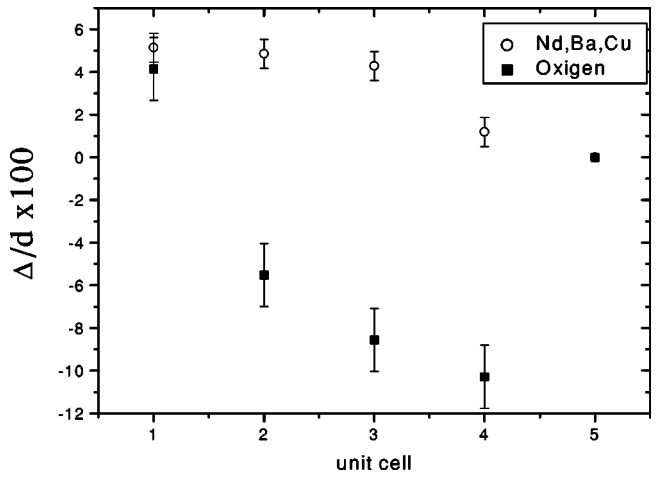

FIG. 12. Average layer displacement from its ideal position obtained from the two termination model best fit for each unit cell corresponding to cation displacements (open circles) and oxygen displacements (filled squares). d is the interlayer distance of the NBCO unit cell ($a_3/6$) and Δ the variation with respect to this value.

D. Surface reconstruction and final remarks on the structural model

Our structural models do not include any contribution from the $c(2\times2)$ surface reconstruction. One of the reasons for such a simplification in our analysis is related to the lower intensities of fractional order rods compared to the CTR's ($I_{fractional}/I_{CTR}=4\%$). However the experimental data (e.g., Figs. 6, 8, and 9) show additional weak reflections between Bragg peaks that cannot be reproduced from a simple surface termination analysis. These extra peaks are

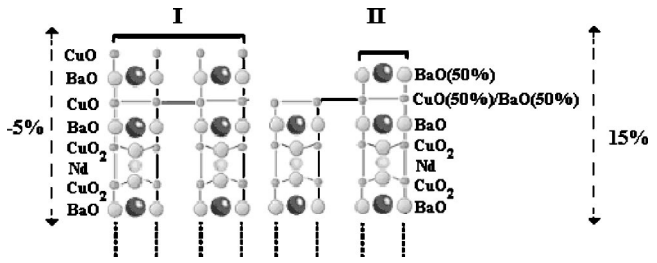

FIG. 13. A schematic diagram of the surface structure which emerges from the two termination model: on the left a complete Cu(1)-O terminated surface with the second layer being BaO; on the right the topmost layers of the second terrace being a partially filled (50%) BaO terrace. The second layer of this terrace is CuO terminated where Ba atoms are substituting Cu atoms in a random way (50:50). Note that the complete Cu(1)-O layer is contracted while the other is strongly relaxed.

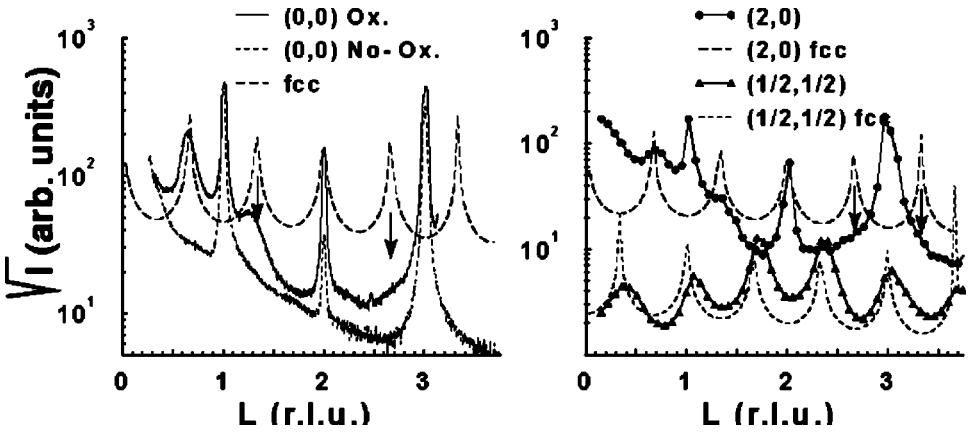

FIG. 14. *l*-scan of different integer and fractional order reflections showing the peaks due to the $c(2\times2)$ superstructure: (a) experimental (0,0) specular integer rod intensity of the oxygen treated sample (continuous line), not treated, air exposed, sample (short dashed line) and calculation for a fcc lattice (long dashed line); (b) (2,0) integer (black line+filled circles) and $(\frac{1}{2},\frac{1}{2})$ (black line+filled triangle) fractional order rods compared to calculations for a fcc lattice corresponding to the (2,0) fcc rod (long dashed line) and $(\frac{1}{2},\frac{1}{2})$ (fcc) fractional rod (short dashed line). The peak placed at 2/3, indicated by the arrow, in the specular rod shows clearly the structural differences between the fresh and the oxygen treated (reconstructed) film.

due to the $c(2\times2)$ reconstruction of the surface. In order to prove that, in Fig. 14(a) we compare the experimental intensity profile of the specular (0, 0) rod of the oxygen treated (reconstructed) sample with that of an identical sample exposed to air. The intensity profiles calculated for a fcc (face centered cubic) $c(2\times2)$ reconstruction is superimposed to the data (dashed lines). In Fig. 14(b) the measured intensity of the (2 0) integer and $(\frac{1}{2},\frac{1}{2})$ fractional order rods are compared with a simple calculation for a fcc lattice. Figure 14 proves that the observed extra peaks in the CTR's, as well as the peaks of the $(\frac{1}{2},\frac{1}{2})$ fractional order rod, are due to the $c(2\times2)$ reconstruction. If we assume that this reconstruction arises from an ordered fcc distribution of vacancies at the surface, we should assign these types of vacancies to oxygen atoms since a distribution of cation vacancies on the surface would introduce strong modulations along the CTR's that are not observed in the experimental data. Moreover, the $c(2\times2)$ reconstruction extends to a minimum of three surface unit cells in depth as deduced from the indexing of the surface peaks that are observed in the integer as well as fractional order rods [Fig. 14(b)]. From these results we conclude that oxygen atoms are probably the main ones responsible for the $c(2\times2)$ reconstruction in the NBCO film, and consequently a different behavior of their atomic displacements with respect to those of cations would be expected.

The disagreement between data and the best fit are exclusively due to the fact that the $c(2\times2)$ superstructure has not been taken into account during the fit refinement procedures, but an approximated average estimation of it instead, since a model with a $p(1\times1)$ unit cell has been considered. The regions in the CTR's, where the $c(2\times2)$ superstructure contributes with stronger peaks as in $l=2/3$ of the (1,1) and (2,0) experimental results, are not well reproduced. The (2,0) rod also shows another $c(2\times2)$ peak at $l=4/3$, better resolved in Fig. 14(b). Other examples where these discrepancies are clearly visible are in the (1,0) rod around the $l=4/3$ and $l=10/3$ $c(2\times2)$ superstructure contributions. The $p(1\times1)$ model used to fit the CTR's only takes into account the average relaxations of the atoms in the superstructure cell but not the most likely fcc-ordering of anion atoms in the superstructure which are responsible of the appearance of these peaks. However the simplification of the models does not affect the main outcomes of the fit concerning surface termination and cation relaxation. On the contrary oxygen rumpling obtained from the fits is strongly affected by the oversimplification of the model which does not consider the $c(2\times2)$ reconstruction (likely due to oxygen vancancies). Consequently the oxygen displacement in Fig. 10 and Fig. 12 should be considered with caution.

V. DISCUSSION

In the previous sections we have compared the experimental results obtained from STM and Gracing Incidence X-ray Diffraction with structural models of NBCO films. The relevant information that can be obtained from the CTR's analysis have been discussed by introducing a gradually different level of complication. It has been shown that the analysis of the CTR's data is sensitive to surface cation relaxation and surface termination since these parameters strongly modify the calculated structure factors.

Two structural models are able to fit the experimental results. In both cases, the picture of the surface structure is quite complex. The surface composition obtained from the refined models shows a similar mixed CuO and BaO termination with a Cu/Ba ratio at the interface with vacuum very close between them (2.3 and 1.7, respectively). However major structural differences between the two models, in terms of the surface cell size, are clearly manifest. The single termination model needs a stack of nine surface cells to progressively reduce to zero the expansion of the topmost surface

atoms. The two termination model also shows an expansion at the topmost surface layers, but it is 3–4 times smaller and consequently concerns four unit cells only. Moreover, the picture emerging from this model is much more consistent with the STM results: the surface presents ordered Cu(1)-O terraces mixed with disordered Cu(1)-O layers characterized by a high percentage of Ba substitution (50%) and covered by an incomplete (50%) BaO layer. Both terraces are very flat and separated by 0.4 nm steps between them which corresponds to Cu-Cu interlayer separation distances (the distance between the topmost filled layers), even though multiple steps are also found (the topmost BaO incomplete layer).

Since both models are based on similar surface structure and composition, the worst agreement with the experimental data of the single termination model is only due to the different way the contribution to the CTR's intensities due to the CuO or BaO layers on the surface are added. The results derived from this comparison force the atomic relaxations of the single termination model to be excessively high since all ideal NBCO terminations produce high asymmetries in the shape profile of some of their calculated CTR's peaks which are not experimentally observed (Fig. 6). This asymmetry is reduced through the introduction of strong atomic relaxations along the surface normal direction.

Finally it is also quite evident that in both models oxygen relaxations play a non-negligible role during the fit refinement procedure that show a different trend from those of cations (Figs. 10 and 12). However, the oxygen displacements should be interpreted with care since they could be an artifact of the fit due to the omission of the $c(2\times2)$ superstructure contributions during the fitting procedure. This superstructure would be compatible with an oxygen vacancy distribution that of course has not been considered during the fitting procedure, and consequently could introduce wrong estimations in their relaxations. These errors would not be expected when determining the cation positions because their atomic number is higher and the experimental data have shown a higher sensitivity to them.

VI. CONCLUSIONS

In this paper we present experimental results on the surface structure and morphology of $Nd_{1+x}Ba_{2-x}Cu_3O_y$ films deposited on $SrTiO_3$ substrates. The experimental data include LEED, GIXD and STM measurements. These techniques provide unique information about the terminating layer of our films. A refined structural model of the surface and of the interface between the bulk and the surface of our film has been obtained.

There was a long debate about the last atomic layer of RBCO films and the differences with single crystals. The answer to this question in the case of the $Nd_{1+x}Ba_{2-x}Cu_3O_y$ films deposited by dc magnetron sputtering on STO substrate is that the surface mainly shows two different types of terraces: an ordered Cu(1)-O plane and a disordered Cu(1)-O one which is partially substituted and covered by a BaO layer. We can compare this result with the study of the YBCO terminating layer inferred by other experiments. Angle resolved x-ray photoemission measurements on YBCO single crystals show that the relative intensity of Ba peaks tends to increase toward the surface.[21] LEED measurements on *c*-axis films, however, indicate that the YBCO lattice reconstruction is due to the ordering of the oxygen in the Cu(1)-O plane.[4] In particular different kinds of reconstruction, like $p(2\times2)$ and $p(1\times4)$, are observed depending on the kind of annealing procedure used to cool the sample. Also Low Energy Ion Surface Scattering (LEISS) give further evidence for a Cu(1)-O plane termination with the second outermost layer being BaO.[22]

Only a few studies have been performed on the NBCO system. Using atomic resolved STM images carried out on NBCO stoichiometric single crystals, Ting *et al.*[23] have shown that air cleaved, and subsequently annealed crystals show structures compatible with a Cu(1)-O terminated surface, characterized however by various kinds of defects.

To the best of our knowledge the use of the GXID technique has been applied to the structural refinement of superconducting cuprate materials or complex perovskite structures only in a few cases. Francis *et al.* have studied the low and high temperature surface structure of $LaAlO_3$ single crystals.[24] Following an approach very similar to ours, they were able to determine surface termination and ion displacements (both in plane and out of plane) of the low and high temperature $LaAlO_3$ phases. Until now only few studies employing GIXD have been reported for RBCO compounds. One of the most interesting result concerns the study of YBCO single crystal performed by You *et al.*[25] Their experiment is very similar to ours, with some important differences. Indeed in both cases CTR's measurements have been fitted using a structural model, however they essentially performed an *ex situ* experiment, without any kind of surface cleaning. The surface of their crystal does not exhibit a surface reconstruction, while our samples are reconstructed. Hue *et al.* found a yttrium termination layer. Since it is well known that a charged surface cannot be stable, they claimed that charge neutralization is guaranteed by an oxygen layer. Our results are strongly in contrast with those obtained by Hue *et al.*, but are in reasonable agreement with the *in situ* investigations performed by LEISS,[22] LEED[4] and angle resolved XPS.[21] Moreover our results agree well with energy minimization calculations performed for the YBCO compound, which show that Cu(1)-O chain and BaO layers are the most stable layers[26] in this material. We believe that the differences between our results and that obtained by You *et al.* can be ascribed to the reaction of the YBCO crystal surface with atmosphere, which can lead eventually to the formation of a $BaCuO_x$ amorphous overlayer. This overlayer is not detected by x-ray diffraction. However we do not rule out the possibility of differences in the termination between single crystals and thin films. GIXD experiments on high quality YBCO and NBCO crystals in UHV conditions with a previously cleaned surface are needed to elucidate this point.

Finally we wish to underline that the agreement between the surface termination of our Nd-rich NBCO films and YBCO films is quite remarkable, since the growth mode of these two compounds is totally different.[5] However it is

noteworthy that Nd-rich films are characterized by a $c(2\times2)$ reconstruction, while stoichiometric samples exhibit typically a $p(2\times2)$ reconstruction. An explanation of this result requires a detailed knowledge of the surface structure of both kinds of materials. In the case of the Nd-rich film we found evidences that the reconstruction is due to the oxygen reorganization in the unit cell. Similar conclusions have been obtained in the case of YBCO films deposited by sputtering.[4] Since the oxygen ordering in the NBCO system is strongly influenced by the Nd-excess, it is plausible that the differences arise from the different reorganization of oxygen ions, which depends on the Nd-content. This point deserves further investigations by carefully comparing the surface structure of stoichiometric and Nd-rich NBCO films.

ACKNOWLEDGMENTS

The present work has been partially supported by the CIPE A3, 5% CNR Projects and the D.G.E.S. (M.E.C.) Project No. PB98-0483. The staff of the ID32 beamline at the ESRF is gratefully acknowledged for technical help during the experiment and for the sample preparation. The authors are grateful to F. Miletto Granozio, G. V. Tendeloo, and S. Bals for useful discussions and suggestions on data interpretation.

*Present address: Pirelli Labs, viale Sarca 222, 20126 Milano.
†Corresponding author. Electronic address: Salluzzo@na.infn.it

[1] T. Terashima *et al.*, Phys. Rev. Lett. **65**, 2684 (1990).
[2] H. P. Lang, Physica C **194**, 81 (1992).
[3] Y. Sakisaka, T. Komeda, T. Maruyama, M. Onchi, H. Kato, Y. Aiura, H. Yanashima, T. Terashima, Y. Bando, K. Iijima, K. Yamamoto, and K. Hirata, Phys. Rev. B **39**, 2304 (1989).
[4] H. Behner, W. Rauch, and E. Gornik, Appl. Phys. Lett. **61**, 1465 (1991).
[5] M. Salluzzo, C. Aruta, I. Maggio-Aprile, Ø. Fischer, J. Zegenhagen, and S. Bals, Phys. Status Solidi A **186**, 339 (2001).
[6] M. Salluzzo, I. Maggio-Aprile, and Ø. Fischer, Appl. Phys. Lett. **73**, 683 (1998).
[7] M. Salluzzo, I. Maggio-Aprile, and Ø. Fischer, IEEE Trans. Appl. Supercond. **9**, 1856 (1999).
[8] S. Bals, G. Van Tendeloo, M. Salluzzo, and I. Maggio-Aprile, Appl. Phys. Lett. **79**, 3660 (2001).
[9] J. Zegenhagen, T. Haage, and Q. D. Jiang, Appl. Phys. A: Mater. Sci. Process. **67**, 711 (1998).
[10] M. Badaye, F. Wang, Y. Kanke, K. Fukushima, and T. Morishita, Appl. Phys. Lett. **66**, 2131 (1995).
[11] P. Yossefov, G. E. Shter, G. M. Reisner, A. Firedman, Y. Yeshurun, and G. S. Grader, Physica C **275**, 299 (1997).
[12] F. Miletto Granozio, M. Salluzzo, U. Scotti di Uccio, I. Maggio-Aprile, and Ø. Fischer, Phys. Rev. B **61**, 756 (2000).
[13] T. Ohara, K. Sakura, M. Kamishiro, and T. Kobayashi, Jpn. J. Appl. Phys., Part 2 **30**, L2085 (1991).
[14] R. Emch, Ph. Niedermann, P. Descouts, and Ø. Fischer, J. Vac. Sci. Technol. A **6**, 379 (1988).
[15] I. Maggio-Aprile, Ph.d. thesis, Université de Genève.
[16] F. Comin, Rev. Sci. Instrum. **66**, 2082 (1995).
[17] M. J. Kramer, S. I. Yoo, R. W. McCallum, W. B. Yelon, and H. Xie, P. Allenspach, Physica C **219**, 145 (1994).
[18] E. Vlieg, J. Appl. Crystallogr. **33**, 401 (2000).
[19] E. Vlieg, J. Appl. Crystallogr. **30**, 532 (1997).
[20] I. K. Robinson, Phys. Rev. B **33**, 3830 (1986).
[21] M. Abrecht, T. Schmauder, D. Ariosa, O. Touzelet, S. Rast, M. Onellion, and D. Pavuna, Surf. Rev. Lett. **7**, 495 (2000).
[22] T. Nakamura, S. Tanaka, and M. Iiyama, Appl. Phys. Lett. **66**, 3362 (1995).
[23] Wu Ting, N. Koshizuka, and S. Tanaka, Appl. Phys. Lett. **72**, 2035 (1998).
[24] R. J. Francis, S. C. Moss, and A. J. Jacobson, Phys. Rev. B **64**, 235425 (2001).
[25] H. You, U. Welp, G. W. Crabtree, Y. Fang, S. K. Sinha, J. D. Axe, X. Jiang, and S. C. Moss, Phys. Rev. B **45**, 5107 (1992).
[26] R. C. Baetzold and J. Mir, J. Cryst. Growth **135**, 145 (1994); F. Miletto Granozio and U. Scotti di Uccio, J. Alloys Compd. **251**, 56 (1997); F. Miletto Granozio and U. Scotti di Uccio, J. Cryst. Growth **174**, 1 (1997).